

# Investigating UHPC in deck bulb-tee girder connections, part 2: Full-scale experimental testing

Abdullah Haroon, Eric Steinberg, Richard Miller, Bahram Shahrooz, and Waleed Hamid

- The research presented in this paper is the experimental testing portion of a larger study performed under National Highway Research Program project 18-18. To enable wider adoption of deck bulb-tee girder systems, design guidelines and standard details must be developed for joints used in these systems to ensure that these joints perform adequately and are useful for accelerated bridge construction.
- This paper, part 2, presents full-scale experimental testing performed as a follow-up to the analytical investigation that appeared in part 1. Longitudinal joints of a deck bulb-tee girder system grouted with ultra-high-performance concrete were tested under thermal and fatigue loading. The longitudinal joint system was also subjected to camber differential between adjacent girders. In addition, a continuity joint composed of conventional concrete and ultra-high-performance concrete was tested for positive and negative moments at the pier.

**P**refabricated bridge elements and systems are an essential part of accelerated bridge construction because they offer significant time and cost savings, improved safety, and convenience for public travel. Precast, prestressed concrete deck bulb-tee girders are one such system because the top flange of the precast concrete girder section can act as the deck of the bridge, which eliminates the need for time-consuming forming, casting, and curing of a cast-in-place deck. These girders are manufactured in precast concrete plants under closely controlled and monitored conditions, transported to the construction site, and erected so that flanges of adjacent units join together. The wide upper flange of deck bulb-tee girders results in a very efficient section for prestressing purposes because it provides a large cross-sectional area that can resist the prestressing force of many strands. The casting of the deck as part of the girder also allows for a variation of the deck thickness, resulting in a more efficient transverse design of the deck.

Despite the many benefits of deck bulb-tee girder bridge systems, their use has been limited and most existing bridges of this type have relatively short spans with low traffic volumes. Concerns regarding the long-term performance of longitudinal and transverse connections between individual girders partially explain why these systems have not been widely used. In addition, variable camber profiles of the girders can cause bridge deck profile problems as the cambers in adjacent girders do not align, making it difficult to make the connection between flanges. Forces are induced

into the system if a leveling procedure is used to remove differential camber between the girders.

Several longitudinal joint details have been proposed and used in deck bulb-tee girder systems. These details can be primarily categorized as follows:

- a bar or plate field welded across the width of the joint and spaced along its length
- distributed reinforcement protruding transversely along the length of the joints.

Because the field-welded connections are widely spaced, limited moment transfer takes place along the joint. Cracking of the joint interface between the grout and girder concrete has been reported.<sup>1-3</sup> The cracking and resulting leakage led the state of Washington to restrict the use of deck bulb-tee girders for bridges with high levels of average daily traffic and for continuous bridges.<sup>4</sup>

Li et al.<sup>4</sup> investigated two distributed joint reinforcement details for deck bulb-tee systems. One detail consisted of a single row of headed bars at the middepth of the flange. The headed bars had lap lengths of 6, 4, and 2.5 in. (150, 100, and 63.5 mm) and bar spacings of 6 and 4 in. The other detail consisted of welded wire reinforcement with spacings of 6 and 4 in. The results showed that the headed-bar detail provided enough force transfer to reduce joint width. French et al.<sup>5</sup> investigated a U-bar detail and a headed-bar detail for the longitudinal connection in deck bulb-tee girders. The U-bar detail consists of a single row of bars bent at 180 degrees with a lap length of 6 in. The headed-bar detail had two rows of smaller headed bars and a lap length of 6 in. The results showed that the U-bar detail with no. 5 (16M) reinforcing bars spaced at 4.5 in. (114 mm) and a 6 in. overlap provided a viable detail. However, the bend diameter of the no. 5 bars for this detail does not meet the minimum bar-bend-diameter requirements of the American Concrete Institute's *Building Code Requirements for Structural Concrete (ACI 318-19) and Commentary (ACI 318R-19)*.<sup>6</sup> Other concerns that have been raised about this detail include loops not fitting correctly, especially on skewed bridges; interference; longitudinal bars not fitting through the loops; and the breakage of the flange tips. It should also be noted that none of the studies described herein considered the thermal loading effects of the connection performance. Several studies<sup>7-9</sup> on box-girder bridges have shown that the girder connections develop higher stress due to thermal loads than the vehicular live load.

Leveling of the differential camber for adjacent beams may be required because camber is inherently inconsistent due to variations in the properties and fabrication dates of components. Differential camber will occur for girders in skewed bridges, even if all components have the same camber profile, because the ends of the girders are offset by the skew distance. Camber differential was reported as one of the most common concerns in a survey regarding the use of deck bulb-

tee girders.<sup>5</sup> Composite decks and concrete overlay can be used to smooth the camber differential, but this work extends the project timeline, defeating the purpose of using deck bulb-tee girder systems to accelerate bridge construction.

The selection of the appropriate joint material is critical for the long-term durability of the joints. The typical practice is to use a nonshrink grout as the joint material since it prevents the shrinkage tension cracking in joints or at the interface. For adjacent box girders, the use of ultra-high-performance concrete (UHPC) as the joint material has been associated with superior-quality shear strengths with relatively short development lengths for any reinforcement extending into the joint.<sup>10</sup> Developed in recent decades, UHPC is a new class of cementitious composites that have improved strength, tensile ductility, excellent bonding properties, and low permeability. The steel fibers in UHPC make it ductile under flexural tension, with the direct tensile strength of the mixture reaching up to 2 ksi (14 MPa).<sup>11</sup> The fibers also help reduce the permeability of the strained section by changing the cracking pattern from fewer wider cracks to several narrower cracks.<sup>12</sup> Using UHPC as the closure pour material in deck bulb-tee girder system connections can improve system performance. Field-cast UHPC joints have been shown to perform better and are more durable than conventional concrete joints.<sup>13</sup>

In multispan applications, the transverse continuity joint between the deck bulb-tee girders is typically made using a cast-in-place diaphragm to connect the girders over the pier. However, this method requires a large transverse joint to fully develop the continuity reinforcement. Also, the use of cast-in-place conventional concrete results in a joint section that has less strength and durability than the rest of the girder. Thus, UHPC may be a useful alternative to cast-in-place concrete for transverse joints. In particular, the use of a conventional-strength diaphragm with a UHPC topping in the top-flange area may provide an economical detail.

Currently, there are no design specifications in the United States for the use of UHPC connections. To date, the most helpful guidance document regarding UHPC connection design is *Design and Construction of Field-Cast UHPC Connections*, published by the Federal Highway Administration in 2014.<sup>13</sup> To enable wider adoption of deck bulb-tee girder systems, design guidelines and standard details must be developed for joints used in these systems to ensure that these joints perform adequately and are useful for accelerated bridge construction.

The research presented in this paper is the experimental testing portion of a larger study performed under National Highway Research Program project 18-18. The analytical findings presented by Haroon et al.<sup>14</sup> guided the direction of the full-scale experimental testing program presented herein, in which the longitudinal joints of a deck bulb-tee girder system were tested when subjected to thermal and fatigue loading and camber differential between adjacent girders. A continuity joint composed of conventional concrete and

UHPC was also tested for positive and negative moments at the pier.

## Experimental program

The experimental testing consisted of the following tasks:

- full-scale experimental testing on a system of three girders (girders 1, 2, and 3) with longitudinal UHPC joints subjected to thermal and fatigue load
- full-scale experimental testing on a system of three girders (girders 1, 4, and 3) with longitudinal UHPC joints subjected to differential camber
- full-scale experimental testing of the transverse joint (continuity connection) between two girders using a partial UHPC connection

## Girder design and fabrication

The test girders were designed based on the ninth edition of the American Association of State Highway and Transportation Officials' *AASHTO LRFD Bridge Design Specifications*.<sup>15</sup> Figure 1 illustrates the joint reinforcement detail and the locations of the instrumentation embedded in the girder during construction; complete details of the design can be found in the first part of this article series.<sup>14</sup> The precast concrete economical fabrication deck bulb-tee section was used for the girders. Although a typical deck bulb-tee girder span ranges between 90 and 180 ft (27 and 54.9 m), the test girder span was limited to 55 ft (16.8 m) due to limitations on the laboratory testing floor. Most of the bridges in the experiment have skews under 30 degrees. In the analytical modeling, it was found that the bridges with skew have higher forces; therefore, the test girders were designed to have a 30-degree skew angle. The two layers of transverse no. 5 (16M) reinforcing bar

provided in the top flange were doweled 5.5 in. (140 mm) into the joint to constitute the joint reinforcement. The transverse reinforcement spaced at 6 in. (150 mm) in the beam was offset longitudinally to create a 3 in. (76 mm) reinforcement spacing in the joint. The reinforcement doweled into the joint from the flanges was fanned at the skewed ends to allow for placement without interference.

Four girders (girder 1, girder 2, girder 3, and girder 4) were designed. Girders 1 through 3 each had 10 straight and two harped strands. Girder 4 was designed to have six additional strands to create the difference in camber that would be used during differential camber testing.

The girders were fabricated at the prestressing plant of Concrete Industries Inc. in Lincoln, Neb. During girder fabrication, four vibrating-wire strain gauges were installed in the longitudinal direction at the midspan of each girder to monitor the strains at various stages of the testing program. Three thermistors were also installed along the depth of the web of each girder to measure internal temperature gradient.

## Thermal and fatigue testing of longitudinal joints

This test assessed the effects of temperature and fatigue loading on the longitudinal UHPC joints of the deck bulb-tee girder system.

**Test setup and instrumentation** Girders 1, 2, and 3 were placed adjacent to each other on the laboratory floor. At each end, the girders were simply supported on elastomeric bearing pads 6 in. (150 mm) wide in the longitudinal direction and 24 in. (610 mm) wide in the transverse joints. Load cells were placed under the bearing pads to measure the end reactions of the girders. The vibrating-wire strain gauges and thermistors embedded in the girders during fabrication would

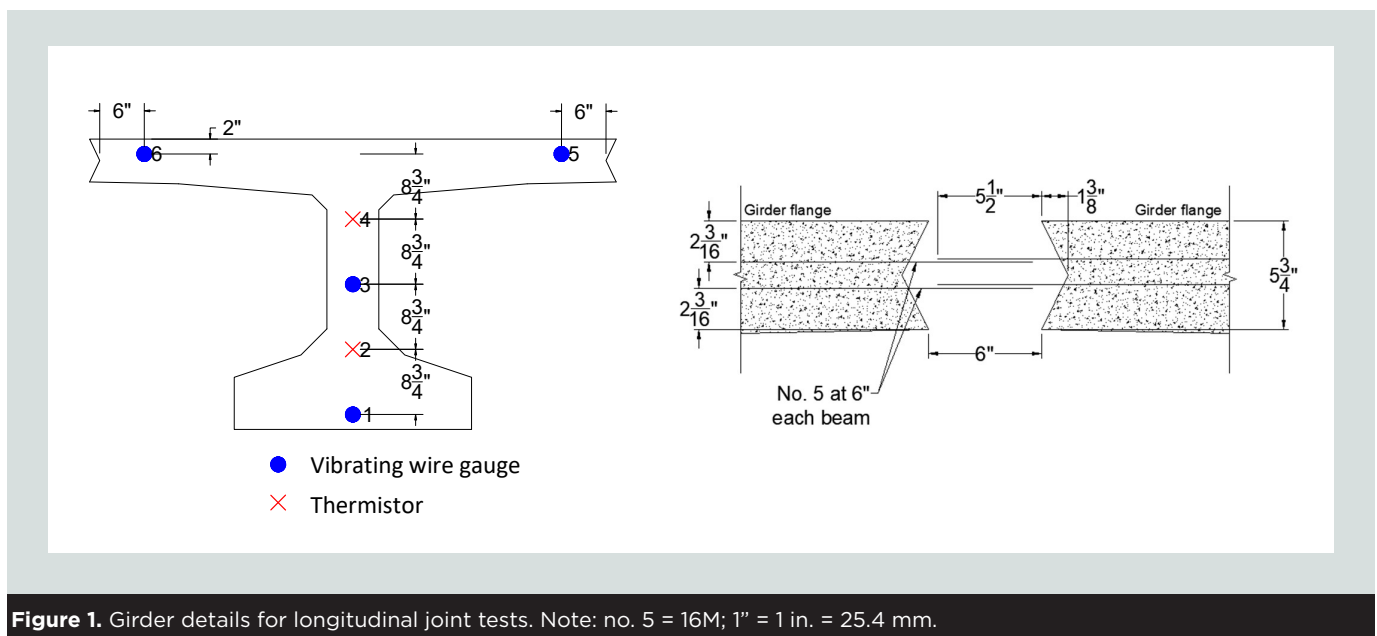


Figure 1. Girder details for longitudinal joint tests. Note: no. 5 = 16M; 1" = 1 in. = 25.4 mm.

be used to monitor temperature profiles and measure strains inside the girder. To measure the girder camber during heating and cooling cycles and during live load tests, linear variable displacement transducers were installed at the midspan of each girder. To measure the lateral movement of the joints due to applied temperature load, 12 in. long (300 mm) vibrating-wire strain gauges were attached on the top surface of the girders such that they spanned across the joints. A total of five vibrating-wire strain gauges were installed on each joint. Since the gauges also have an inbuilt thermistor, they were also used to measure the surface temperature of the girders. A 12 in. long vibrating-wire strain gauge that spanned across the bottom of the joint was also installed at midspan of each joint. To measure the strains in the joints after UHPC was placed, strain gauges were attached to the joint reinforcement bars. Upon placement of the UHPC into the joints, these strain gauges were embedded into the joints and then used to measure the strain in the joints as well as any slip of the reinforcement. The layout of these gauges is shown in Fig. 2.

Figure 3 shows the girder assembly on the laboratory floor. To apply the temperature load, a temperature gradient along the girder depth was to be developed. For this purpose, a closed environmental chamber or “insulated box” was built on top of the girder deck. This methodology was adapted from a paper by Shi et al.<sup>16</sup> A wooden frame was constructed on top of the girders and then covered with 2 in. thick (51 mm) expanded polystyrene foam sheets. The top view of the completed insulated box is shown in Fig. 3. Eighteen 250-watt heat lamps, eight high-capacity heaters, and six circulation fans were installed inside the insulated box. The heat lamps, heaters, and fans were uniformly distributed inside the insulated box and were regulated to generate thermal gradient in the girders.

**Thermal loading of open joints** The thermal properties of concrete vary with the mixture proportions. Therefore, an initial establishment of thermal properties of the girders was

required. The girders were heated and cooled several times before UHPC placement in the joints. Strain, deformation, and thermal response of the individual girders were recorded. This type of evaluation served two purposes:

- It established an appropriate heat cycle protocol that would develop a similar gradient through girder depth, as suggested in the AASHTO LRFD specifications,<sup>15</sup> and that would be used for thermal loading of the girder system. Several trial heating-and-cooling cycles were performed by varying the intensity of the heaters and the locations of the circulation fans until an appropriate gradient was developed in the girders.
- It established the thermal properties of the system, without shear keys, such as the camber of the individual girders and strain across the joints. This information would serve as a reference for the measurements taken after the grouting.

To generate a thermal gradient in the girders, the heat lamps and circulation fans were turned on initially. The heaters were ramped up gradually to heat the top of the surface. The heating equipment was placed to heat the entire top of the girder system as uniformly as possible. The AASHTO LRFD specifications stipulate a temperature gradient  $T_1$  of 38°F (21°C) to 54°F (30°C) between the top of the girder and a position 16 in. (406 mm) deep and a gradient  $T_2$  of 9°F (5°C) to 14°F (8°C) between the depths of 4 in. (100 mm) and 16 in. (Fig. 3). In this artificially simulated heating environment, it was not possible to control the temperatures in both locations simultaneously. The temperature gradient within the girder was critical to the performance of the joints, so the gradient between 4 and 16 in. (gradient  $T_2$  for zone 1) was the key parameter that was monitored during a typical heat cycle. This temperature gradient value marked the peak of the heating, and once this gradient was around 14°F for all the girders, the heat was turned off.

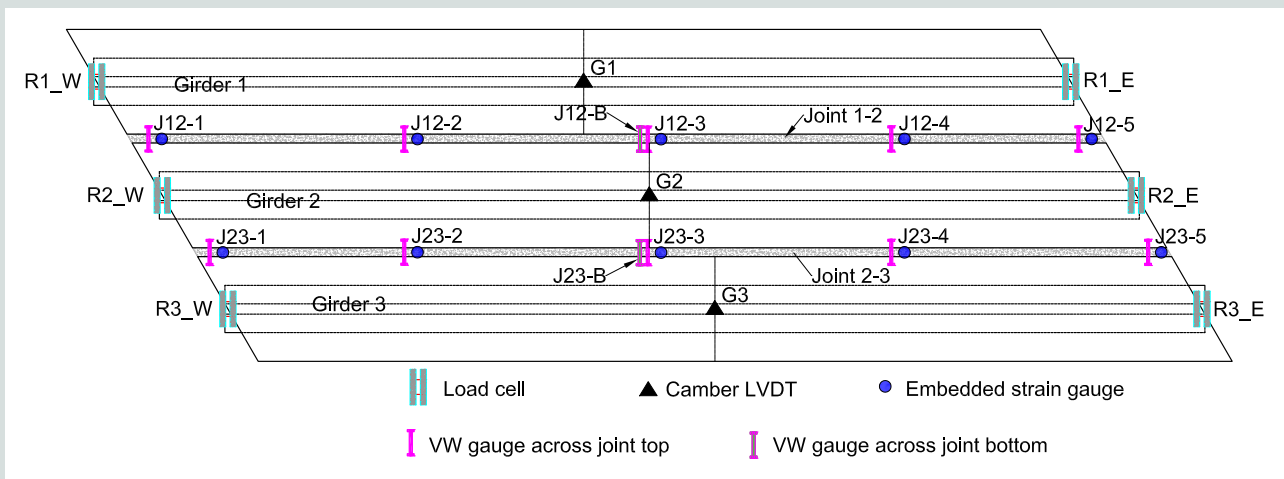
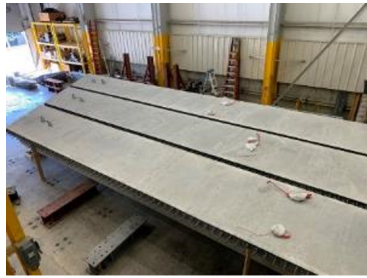


Figure 2. Instrument location and labels for thermal and fatigue testing of longitudinal joints. Note: LVDT = linear variable displacement transducer; VW = vibrating wire.



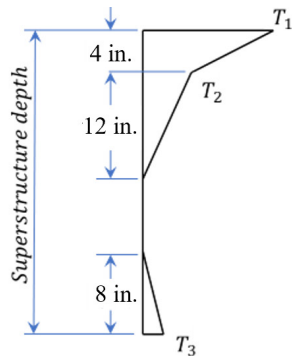
Test girders on laboratory floor



Construction of wooden framing for insulation box



Top view of the completed insulation box



Zone	$T_1(^{\circ}F)$	$T_2(^{\circ}F)$
1	54	14
2	46	12
3	41	11
4	38	9

AASHTO temperature gradient



Inside view of the insulation box

**Figure 3.** Test setup for thermal and fatigue load test for longitudinal joints. Note: AASHTO = American Association of State Highway and Transportation Officials,  $T_1$  = thermal gradient between girder surface and 16 in. depth;  $T_2$  = thermal gradient between 4 and 16 in. depths. 1 in. = 25.4 mm;  $^{\circ}F = 1.8(^{\circ}C)$ .

**Figure 4** shows the camber of the girders alongside the gradient at a depth of 4 in. (100 mm) during a typical heating cycle. As expected, all the girders cambered up with an increase in the girder temperature gradient and cambered down as the girders cooled. Girders 1 and 2 had almost the same maximum camber of approximately 0.13 in. (3.3 mm), whereas the maximum camber for girder 3 was about 0.2 in. (5 mm). This variation in the cambers of the girders was expected given the concrete variability. Figure 4 shows the strain across the tops and bottoms of the joints alongside the average girder temperature gradient before grouting. Both the tops and bottoms of the joints showed a compressive strain as the girder temperature gradient, indicating that the girder flanges were expanding and the joint was closing. The tops of the joint (gauges J12-3 and J23-3) developed higher compressive strain than the bottoms of the joint (gauges J12-B and J23-B).

Figure 4 shows the temperature profiles through the depth of girder 2 at various times during a typical heat cycle. At the start of heating, the temperature was almost uniform

throughout the girder depth. It took around 8 hours to reach the heating peak (defined by a 14°F [8°C] gradient at a 4 in. [100 mm] depth); at that point, the surface temperature was around 100°F (37.8°C) and the temperature at a depth of 20 in. (510 mm) was almost same as at the beginning of the heating cycle. After 4 hours of cooling, the surface temperature dropped faster than the temperature inside the girder flange. Also, the girder web became slightly warmer than it was at the peak heating.

Figure 4 compares the girder temperature gradient with the gradient band recommended in the AASHTO LRFD specifications. The gradient at 4 in. (100 mm) depth  $T_2$  was in the range of 15°F (8°C) to 16.5°F (9°C) for the three girders. This temperature gradient is above the recommended value of 14°F (8°C) for  $T_2$  in the most extreme AASHTO zone 1 condition. The temperature gradient at the surface of the girders  $T_1$  was between 33°F (18°C) and 40°F (22°C), which was slightly below the range of 38°F (21°C) to 54°F (30°C) recommended in the AASHTO LRFD specifications. However, as discussed,

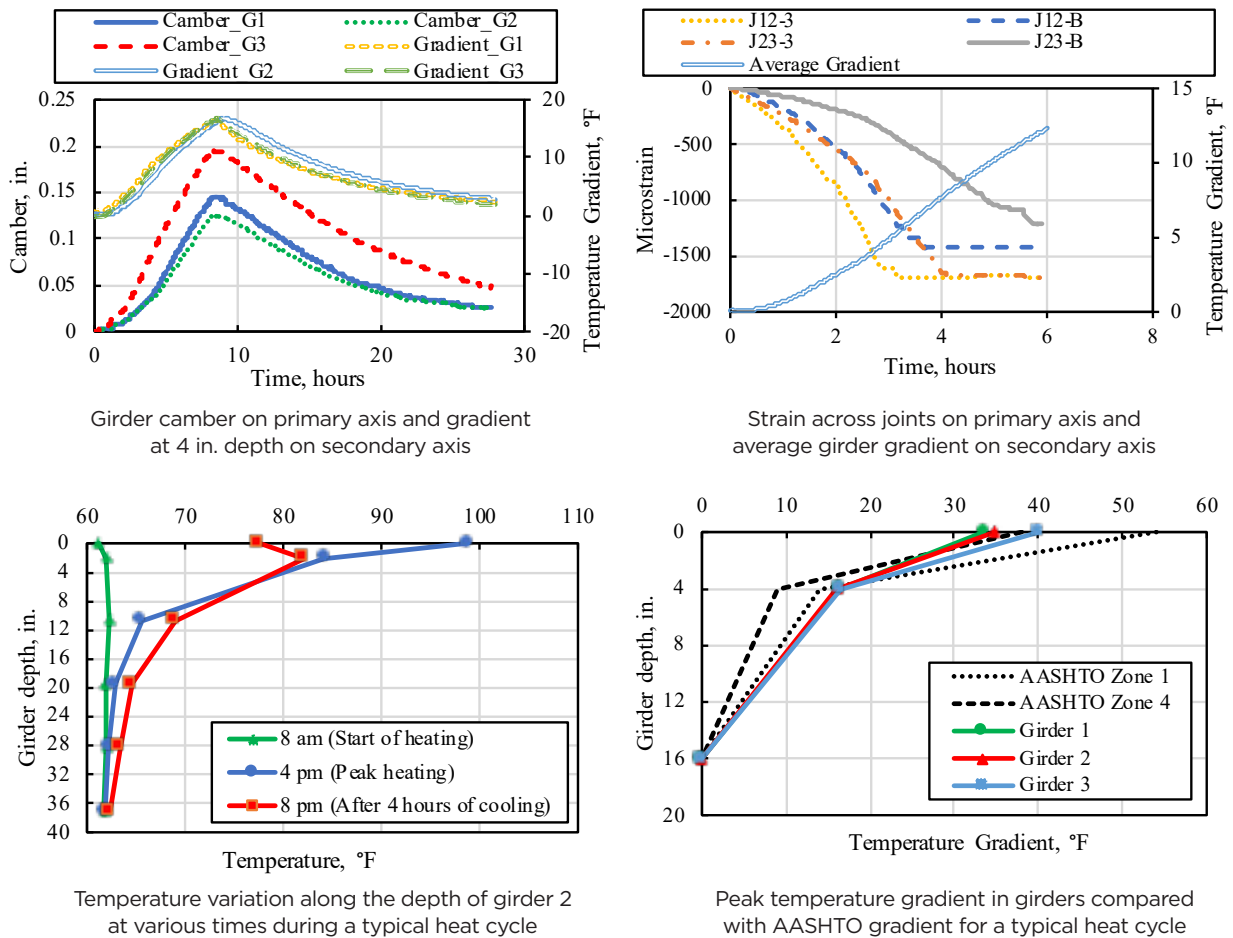


**Figure 4.** Thermal testing of the girder system with open joints before grouting the joints with ultra-high-performance concrete. Note: AASHTO = American Association of State Highway and Transportation Officials. 1 in. = 25.4 mm; °F = 1.8(°C).

under laboratory conditions, it was not possible to control both  $T_1$  and  $T_2$  simultaneously and because  $T_2$  was critical for the performance of the joints, it was selected as a control for the heating cycle.

**UHPC placement in joints** After testing on open joints was completed, formwork was placed at the top and bottom of the joints, and the joints were grouted with UHPC. A proprietary UHPC mixture was used for this project. **Table 1** provides some of the properties of the material used. This commercially available product has been used in numerous projects throughout the United States and was used by the authors in several previous projects. It should also be noted that due to delays caused by the COVID-19 shutdown, the UHPC sat in the laboratory for approximately 1 year before the experiment was conducted. The UHPC seemed to have a slightly more doughy consistency during placement than the authors were accustomed to. **Table 2** presents the UHPC mixture proportions used for this project and the fresh UHPC properties. Slightly higher amounts of water were used because the premixture was approximately 1 year old. A representative of the manufacturer was present and supervised

the mixing; the manufacturer indicated that neither the age of the material nor the additional water put the UHPC out of specification.

To make the UHPC flow along the joints, the joints were covered with formwork both at the bottom and the top. Two openings were made on each joint, and “chimneys” were installed. The UHPC was placed into the joint through these chimneys. To simulate field conditions, the girders were heated the day before UHPC placement and again in the morning of placement to keep the girders as warm as possible during the placement process. When the crew was ready to grout the joints, the ceiling of the insulation box was removed to allow easy access of the joints to place the UHPC. Just before the UHPC was placed into the joints, the top forms were removed and a fine water mist was applied to wet each joint; then the top forms were screwed back into place. The UHPC was transferred from the mixer in buckets into the chimneys, which were placed approximately at third points on the joints (**Fig. 5**). This arrangement allowed the UHPC to flow in each direction. A hydraulic head was maintained in the chimneys to ensure that the entire joint was filled.

**Table 1.** Published properties of the proprietary ultra-high-performance concrete used on this project

Density	150 to 160 lb/ft <sup>3</sup>
Flow	7 to 10 in. diameter without visible sign of fiber segregation
Working time/set time	Approximately 120 minutes/ 15 to 18 hours
Compressive strength*	>14 ksi <sup>†</sup> at 4 days <sup>‡</sup>
	>21 ksi at 28 days
Tensile strength <sup>§</sup>	>725 psi at 28 days
Modulus of elasticity	>6500 ksi at 28 days
Long-term shrinkage	<800 microstrain at 28 days
Chloride ion penetrability	<250 coulomb (very low) at 56 days
Resistance to freezing and thawing	>96% RDM at 300 cycles

Note: Field results may differ depending on mixing/test methods, equipment used, temperature, and site/curing conditions. 1 in. = 25.4 mm; 1 lb/ft<sup>3</sup> = 16.01 kg/m<sup>3</sup>; 1 psi = 6.895 kPa; 1 ksi = 6.895 MPa.

\* Compression tests are performed on 3 × 6 in. cylinders with ends ground flush before testing.

<sup>†</sup> 14 ksi is the typical minimum compressive strength required before application of design live load for most closure pour applications; consult the engineer or project specifications to verify.

<sup>‡</sup> Four days or less is typical when the ambient curing temperature is greater than 60°F (16°C). For colder temperatures, an accelerating admixture may be required to obtain 14 ksi in four days. For 14 ksi compressive strength in 12 to 36 hours, consider using a rapid-set product.

<sup>§</sup> This test measures the sustainable postcracking direct tension strength of a mixture with 2% (by volume) steel fibers.

After sufficient UHPC was placed into the joints, the insulated box was closed, and girders were heated again to regain the lost temperature gradient. Three days later, the forms were removed from the joint. Both joints turned out well. Figure 5 shows the top of the joint between girders 2 and 3 at the west end. The sealer material on each side of the joint was used to ensure that the UHPC did not leak out of the joint and gave an approximately 0.125 in. (3.2 mm) height above the joint. UHPC is often placed approximately 0.125 to 0.375 in. (3.2 to 9.5 mm) higher than the adjoining members in the field and ground flush.

During the UHPC placement, 3 × 6 in. (76 × 150 mm) cylinders were cast for compression testing (Table 3). The 28-day (thermal) results were for cylinders stored within the insulated box built on the girders. Several thermal cycles were performed while these cylinders were inside the box. The purpose of these cylinders was to match the conditions

of the UHPC in the joint. The compressive strength of the UHPC was within the range of the standard specifications for this product.

**Thermal loading after grouting** Starting on the next day after the UHPC placement, thermal loading as described in the previous section was applied to the girder system. Fourteen heating cycles were completed. The girders were heated until the temperature gradient between 4 and 16 in. (100 and 406 mm) below the girder surface reached approximately 14°F (8°C), and then they were allowed to cool until the gradient fell at least below 6°F (3°C). Ideally, the temperature gradient should have been reduced to 0°F (0°C) before the next cycle but cooling the girders to this extent in the enclosed laboratory setup with the heat box on top would have taken a very long time. Also, Miller et al.<sup>17</sup> observed during field monitoring of temperature profiles in box girders that girders hold some heat overnight, so the authors decided to limit the lower temperature gradient to 6°F or less.

Data were recorded from instruments during every thermal cycle. Results of various measurements during the first and fifth heating cycles are discussed herein. The first cycle was critical because the joints were gaining strength during this time. During the fifth cycle, the joints had gained sufficient strength and joint formwork was removed. No significant differences in the measurements were observed between the fifth and final thermal cycles.

During the first cycle, the girder cambers were slightly lower than the cambers recorded before grouting of the joints (Fig. 4). This finding was expected because the joint formwork was still in place during this cycle and would have provided some restraint to the movement of the girders. During the fifth cycle, when the formwork was removed, the girder camber values were the same as the camber values before grouting of the joints. However, the fifth-cycle variation in the camber values of different girders was much lower than variation before grouting of the joints, indicating that the joints had gained strength and the girder system was acting as a unit. For both joints, the strains inside the joints were found to increase from 150 to 250 microstrains during first thermal cycle to 250 to 350 microstrains during fifth thermal cycle; this difference can be attributed to joint formwork being present during the first cycle and absent during the fifth. No obvious signs of reinforcing bar slippage or cracking were observed.

Figure 6 compares the strain across joints 1–2 and 2–3 during the first and fifth thermal cycles. During the first cycle, both joints developed a compressive strain in the range of 300 to 400 microstrains upon heating. Upon cooling, the strains reduced in magnitude but remained compressive. However, during the fifth cycle, the joints developed a compressive strain in the range of 80 to 120 microstrains upon heating and then, upon cooling, the strain became tensile in the range of 0 to 50 microstrains. These findings indicate that during the first cycle, when the UHPC joints were still gaining strength, they allowed the girder flanges to expand and therefore the

**Table 2.** UHPC mixture constituents and fresh UHPC properties for thermal and fatigue testing of the longitudinal joints

		Batch 1 (joint 2-3)	Batch 2 (joint 1-2)
Constituents, lb/yd <sup>3</sup>	UHPC premixture	3690	3690
	Water	216	219
	Fibers	264	264
	Superplasticizer	50.4	51.2
Fresh UHPC properties	Time of mixing	10:33 a.m.	12:49 p.m.
	Laboratory temperature, °F	51	51
	UHPC temperature, °F	70	71
	Static slump, in.	8.75	8.75
	Dynamic slump, in.	9.35	9.25

Note: UHPC = ultra-high-performance concrete. 1 in. =25.4 mm; 1 lb/yd<sup>3</sup> = 0.59 kg/m<sup>3</sup>; °F = 1.8(°C) + 32.

joints developed higher compressive stresses (300 to 400 microstrains). However, during the fifth cycle, when the joints had gained strength, they resisted the movement of girder flanges and therefore the compressive stresses were reduced (80 to 120 microstrains).

**Combined thermal and fatigue loading** After the thermal cycles were completed, cyclic live loading was applied to the girder system. **Figure 7** illustrates the load setup without the insulating box in place. A cyclic load between 0 and 70 kip (0 and 310 kN) was applied at a frequency of 2 Hz. A total of 1 million live-load cycles were applied.

The first 100,000 cycles were applied without thermal loading to monitor any immediate effect of live load after thermal cycles. After the initial 100,000 cycles were completed, thermal loading was also applied during the cyclic live loading (Fig. 7). During each thermal cycle, 100,000 cycles of live load were applied. At the end of each thermal cycle, cyclic loading was stopped and a 70 kip (310 kN) load was applied statically to monitor potential degradation of connection integrity in terms of load distribution or deflection of individual girders. These pauses in the cyclic live-loading process were necessary to read instrumentation, which could not be read during the 2 Hz cyclic



“Chimneys” at third points used to pour UHPC into the joints



Top view of the UHPC joint between girders 2 and 3 after removing the formwork

**Figure 5.** Grouting of the longitudinal joints with ultra-high-performance concrete.

loading. The process continued until 1 million live-load cycles were applied.

The support reactions during static testing before and after the combined thermal and fatigue loading showed no change in the load distribution, indicating that the joints were not degraded by the live-load cycles. The deflections of the girders at the beginning and end of the combined thermal and fatigue loading also showed no change. The maximum strain within the joints due to static load was around 80 microstrain, which is less than the strain developed in the joints due to thermal loading. Again, no significant change in the joint strains was found before or after the live-load cycles. In addition, no obvious signs of reinforcing bar slippage or cracking were observed in either joint.

**Joint flooding and inspection** After the combined thermal and fatigue loading was completed, the joints were visually analyzed. No cracking was visible. However, micro-cracking can be difficult to visually identify; therefore, joints were flooded with water to inspect for any leaks (Fig. 8). Dams were constructed and sealed around the top surface of the joints. These dams were then flooded with water. Flooding revealed severe cracking in joint 1–2 between girders 1 and 2.

**Table 3.** Results of compression testing the ultra-high-performance concrete cylinders made during thermal and fatigue testing

Age, days	Average compressive strength, psi
7	15,465
14	17,348
28	21,749
28 (thermal)	22,384
120	26,039

Note: 1 psi = 6.895 kPa.

Joint 2–3 between girders 2 and 3 had a few small leaks. The leakage occurred both at the interface between the girder and the UHPC and within the UHPC.

Several factors, either individually or in combination, could have caused the cracking. The interface could have dried out during delays in placing the UHPC. However, cracking was found within the UHPC in addition to along the interface.

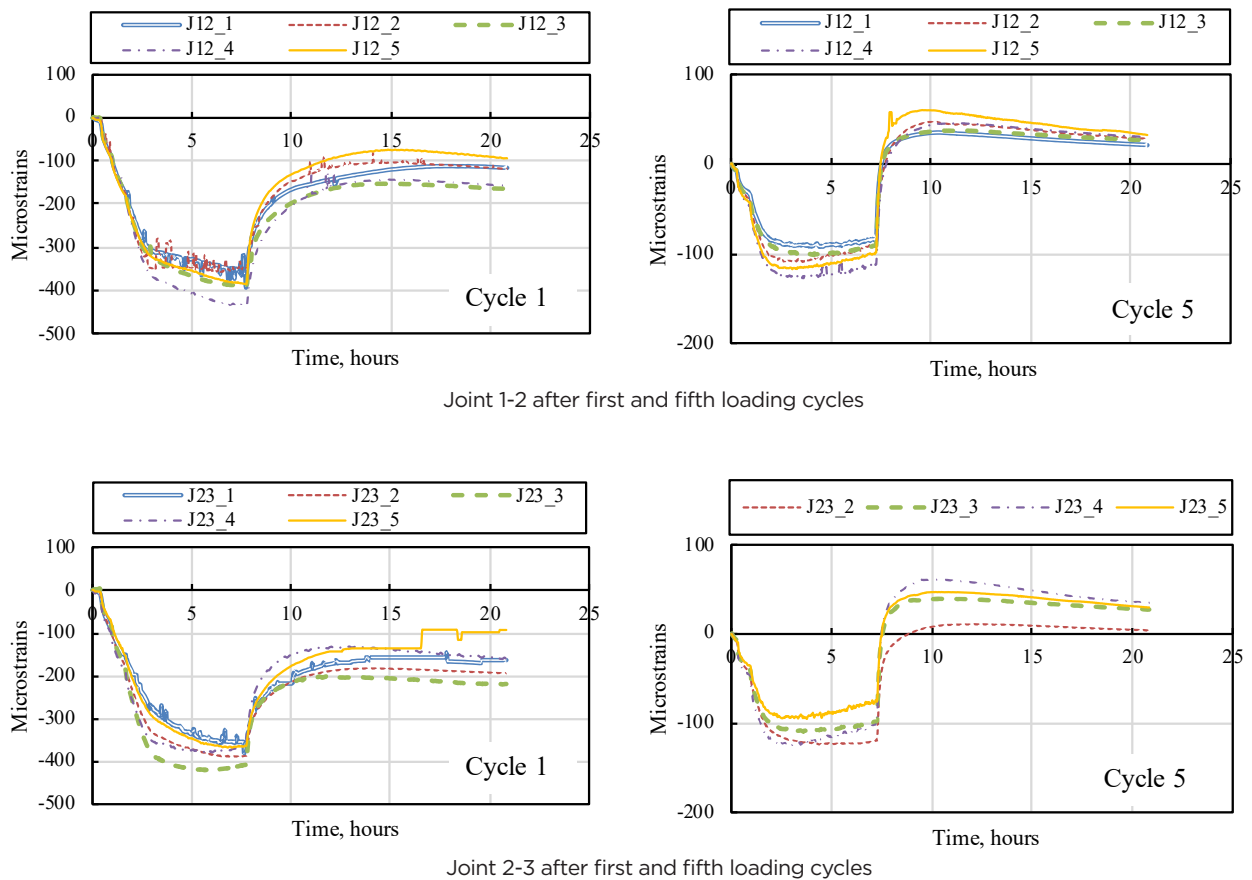


**Figure 6.** Strain across the joints during thermal loading of the girder system after placement of ultra-high-performance concrete in the longitudinal joints.

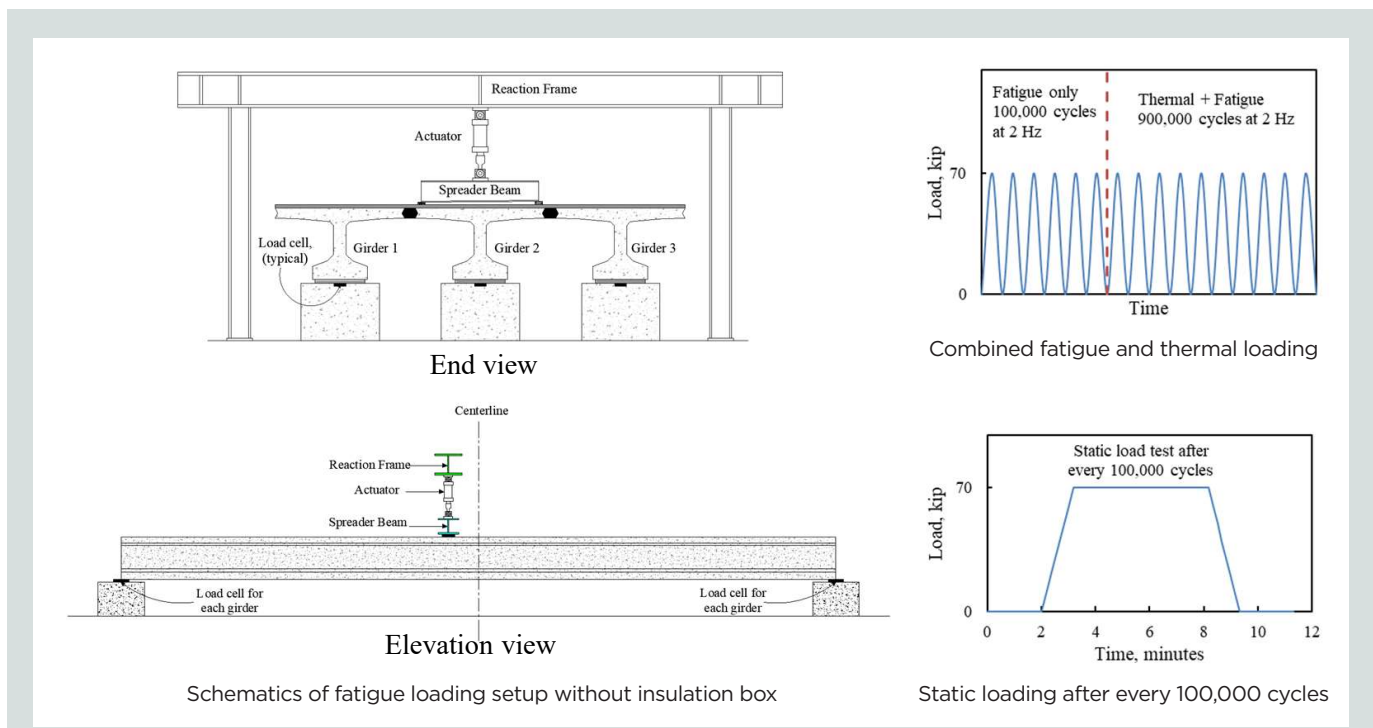


**Figure 7.** Combined thermal and fatigue load setup and loading protocol. Note: 1 kip = 4.448 kN.

Shrinkage of the UHPC during curing could have resulted in cracking along the interface and within the UHPC. Changes in strain measurements during thermal loading may indicate that cracking occurred during the thermal cycle. The thermal cycle loading in this experiment was severe and may not be typically experienced during UHPC placement. Lastly, the UHPC was more than 1 year old when placed. Flow of the UHPC did appear to slow down for the joint that experienced more cracking.

## Differential camber testing of longitudinal joints

Deck bulb-tee girders may have variable camber profiles if their material properties vary or if they are fabricated on different dates. When these girders are erected next to each other, the system may have a camber differential in the adjacent beams. Many contractors employ some type of leveling procedure to minimize the camber differential between adjacent units. The girders are either pulled up or pushed down and jacked in place while the joints are grouted and cured. Any procedure used to remove or reduce the camber differential introduces additional forces in the joints. Tests were performed to evaluate the effect of camber differential between the girders.

**Test setup and instrumentation** After the thermal and fatigue load testing was completed, the girder assembly was cut along the joint lines to disconnect the three girders. Girder 2, the middle girder during thermal and fatigue tests, was now removed from the laboratory floor. Girders 1 and 3 swapped positions so that their exterior sides of flanges not used in ther-

mal testing could now be used. Girder 4 was placed in between girders 1 and 3 to create a new setup with two longitudinal joints. As noted earlier, girder 4 had six additional prestressing strands to ensure that its camber differed from the camber of girders 1 and 3. The measured girder cambers at midspan for girders 1, 4, and 3 were 0.875, 1.375, and 1 in. (22.2, 34.9, and 25.4 mm), respectively. Thus, the differential cambers were 0.5 in. (12.7 mm) between girders 1 and 4 and 0.375 in. (9.5 mm) between girders 4 and 3.

The instrumentation used to monitor the behavior of the joints was same as the instrumentation used in the thermal and fatigue tests, except that the vibrating-wire gauges were now used to record strain only. Because the girder assembly was changed for the differential camber testing, a new scheme of instrumentation labels (**Fig. 9**) was used to be consistent with the changed girder labels and to avoid confusion with the previous scheme of instrumentation.

**Leveling of camber and UHPC placement** The differential camber between girders was removed by loading the middle girder (girder 4) to approximately 90 kip (400 kN). This loading resulted in a downward deflection of 0.5 in. (12.7 mm) for girder 4. The hydraulic cylinder was locked off to hold the girder in position. The loading slightly decreased from seepage of the hydraulic pressure, creep of the girder, and settlement of the system. However, the downward deflection remained at approximately 0.5 in. to match flange heights (**Fig. 10**). Formwork was then attached to the girders and the UHPC was placed. **Table 4** presents the UHPC mixture proportions and fresh properties, and **Table 5** provides the compressive strength of the UHPC.



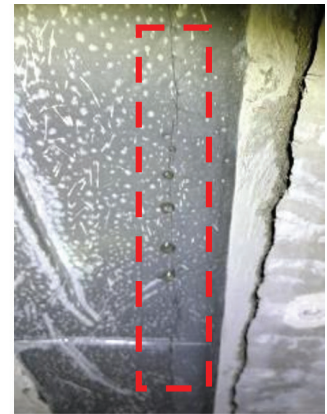
Dams filled with water



Puddles of water leaked from joint between girders 1 and 2



UHPC girder interface leakage



Leakage within the UHPC

**Figure 8.** Joint flooding details.

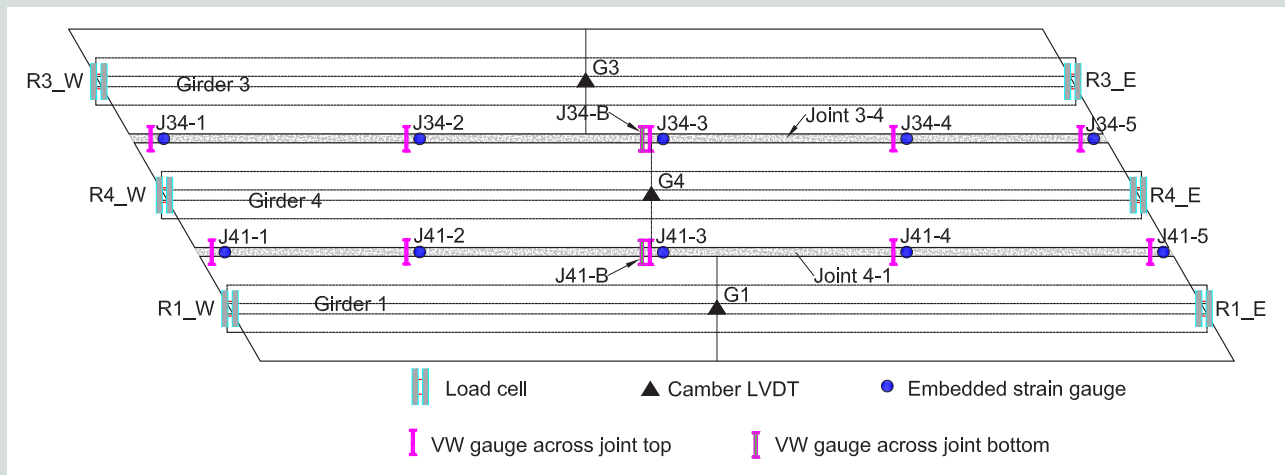


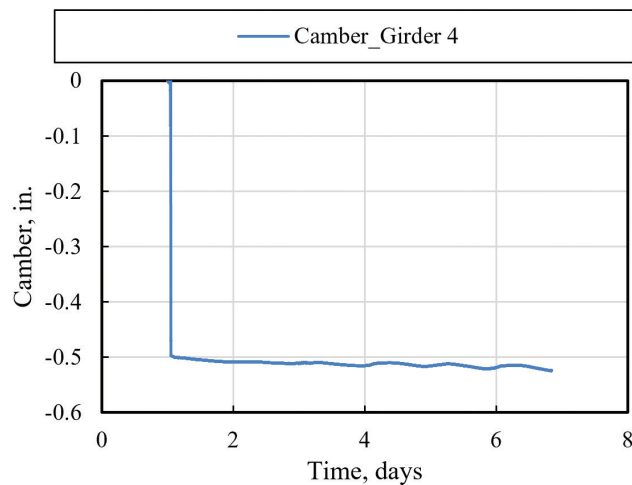
**Figure 9.** Instrument location and labels for differential camber testing of longitudinal joints. Note: LVDT = linear variable displacement transducer; VW = vibrating wire.

**Load release and joint inspection** Three days after UHPC placement, the top forms were removed. Dams were erected around the joints and waterproofed. On the fourth day after UHPC placement, the dams were filled with water for more than 30 minutes. No cracking was observed from leakage of the joint. The load used to remove the differential camber was then released gradually in 15 kip (67 kN) increments. Upon removal of the first load increment, leakage and cracking occurred in joint 3–4 between girders 3 and 4. The cracking occurred within the UHPC as well as within the interface between the UHPC and the girder flanges. The joint 4–1 between girders 4 and 1 also had minor cracking. Most of the cracking occurred on joint 3–4 and mostly in the region where UHPC was placed at the end.

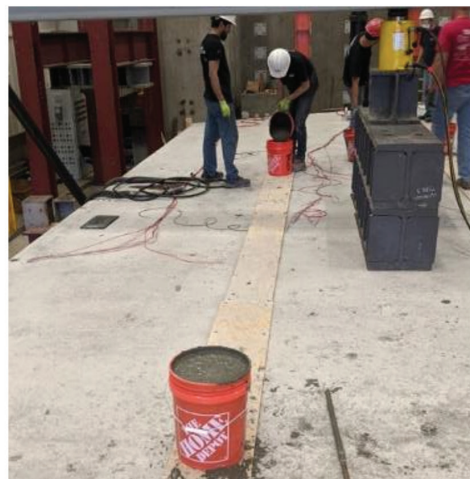
Upon removal of the camber leveling load, girder 4, which had been pushed down by 0.5 in. (12.7 mm) at the midspan

before the UHPC was placed, rose by 0.2 in. (5.1 mm). The midspan of girders 1 and 3 rose approximately 0.12 in. (3.0 mm). Since the cambers were measured at the bottom, this finding implies a slight bending of the flange, a slight rotation of the outside girders, or a combination of slight flange bending and slight girder rotation.

**Fatigue loading** After the load was fully released from the system, cyclic testing of 70 kip (310 kN) was performed. A total of 1 million cycles were applied to the system. At various periods throughout the cyclic loading, the cyclic loading was stopped and a static 70 kip load was applied to investigate any deterioration of the joints due to live load. Several of the static loadings also included flooding the joints. No evidence of new cracks due to cyclic loading was found. The few existing cracks grew by less than 1 in. (25.4 mm).



Deflection of girder 4 during jacking operation



Grouting the joints with ultra-high-performance concrete with jacking in place

**Figure 10.** Differential camber testing of longitudinal joints. Note: 1 in. = 25.4 mm.

**Figure 11** plots the camber data from static load tests before the start of the load cycles and after completion of 1 million cycles of loading. The cambers at the start and end are nearly identical, indicating that the system did not degrade over the loading cycles. Figure 11 plots the support reaction data from the beginning of the experiment and after 1 million cycles of loading. The reactions are also nearly identical, indicating that the system did not degrade.

### Continuity joint testing

The continuity joint design was based on the AASHTO LRFD specifications<sup>15</sup> and results of analytical modeling presented in the first part of this article series.<sup>14</sup> **Figure 12** shows the continu-

ity joint detail tested. UHPC was only used in the upper portion of the diaphragm to save on material costs and deal with the higher negative moment. The lower portion of the diaphragm was conventional concrete. The continuity connection had a positive moment design capacity of 78 kip-ft (106 kN-m) and a negative moment design capacity of 1152 kip-ft (1562 kN-m).

**Test setup and instrumentation** To test the performance of a continuity joint made of UHPC, two 20 ft (6 m) long precast concrete economical fabrication girders were constructed. The girders were placed end to end, 7.5 in. (191 mm) apart. A 1 ft wide (0.3 m) diaphragm was constructed to make the girders continuous. The girders were embedded approximately 2.25 in. (57.2 mm) into the diaphragm. The

**Table 4.** UHPC mixture constituents and fresh UHPC properties for differential camber testing of the longitudinal joints

		Batch 1 (joint 2-3)	Batch 2 (joint 1-2)
Constituents, lb/yd <sup>3</sup>	UHPC premix	3840	3840
	Water	215	215
	Fibers	264	264
	Superplasticizer	50.4	52.6
Fresh UHPC properties	Time of mixing	10:33 a.m.	12:49 p.m.
	Laboratory temperature, °F	75	79
	UHPC temperature, °F	91	91
	Static slump, in.	8.75	8.5
	Dynamic slump, in.	9.75	9.5

Note: UHPC = ultra-high-performance concrete. 1 in. =25.4 mm; 1 lb/yd<sup>3</sup> = 0.59 kg/m<sup>3</sup>; °F = 1.8(°C) + 32.

reinforcement in the diaphragm was provided according to the requirement of continuity joint design. In addition, welded wire mesh (12 × 12 in. [305 × 305 mm]) was placed to prevent shrinkage cracking. The bottom 33 in. (840 mm) of the diaphragm was constructed using conventional concrete. Eleven days after the placement of the concrete, the UHPC was placed only in the top 6 in. (150 mm) of the diaphragm, equal to the depth of the top flange. Figure 12 shows the continuity diaphragm after removal of the formwork. Instrumentation was installed within the joint and on the top reinforcement.

**Positive moment testing** Hydraulic cylinders were placed 12 ft. (3.7 m) from the face of the joint under each girder. A frame was placed over the joint to keep it from moving upward. The hydraulic cylinders were used to apply an upward force, thereby creating a positive moment in the joint. **Figure 13** provides the schematics of the test. A maximum load of 7.3 kip (32.5 kN) was applied, resulting in a positive moment of 87.6 kip-ft (118.8 kN-m) at the joint. Figure 13 shows the strains in the vibrating-wire strain gauges within

**Table 5.** Results of compression testing the ultra-high-performance concrete cylinders made during differential camber testing

Age, days	Average compressive strength, psi
3	10,410
7	15,507
14	17,536
28	20,024

Note: 1 psi = 6.895 kPa.

the joint and the positive moment developed at the joint. The strains were very small. As expected, gauge 1 near the bottom of the connection experienced tension whereas the gauges in the flanges (gauges 4, 5, and 6) experienced compression. No cracking was observed.

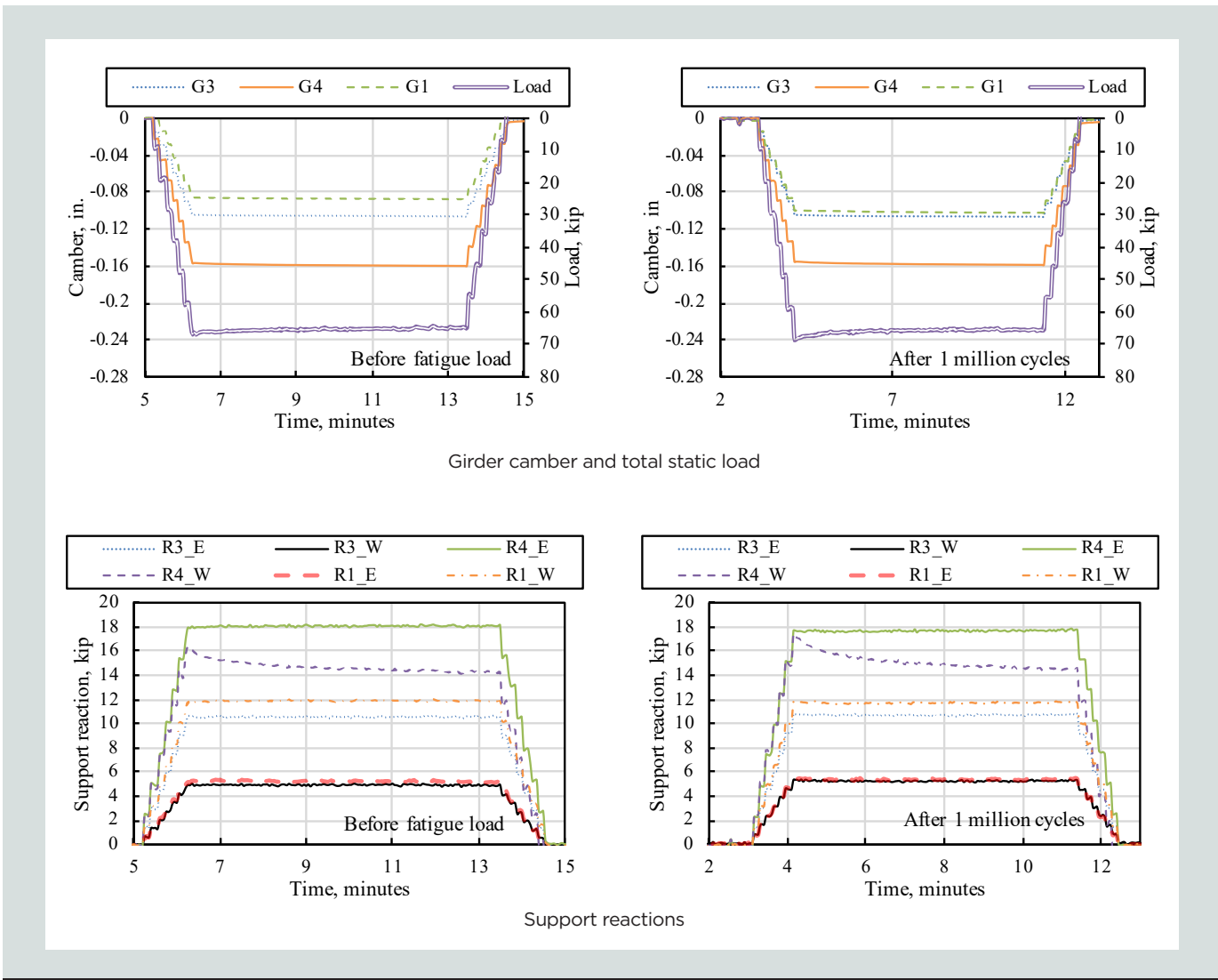


**Figure 11.** Results of static load tests at the beginning and end of the live load cycles for differential camber test. Note: 1 in. = 25.4 mm; 1 kip = 4.448 kN.

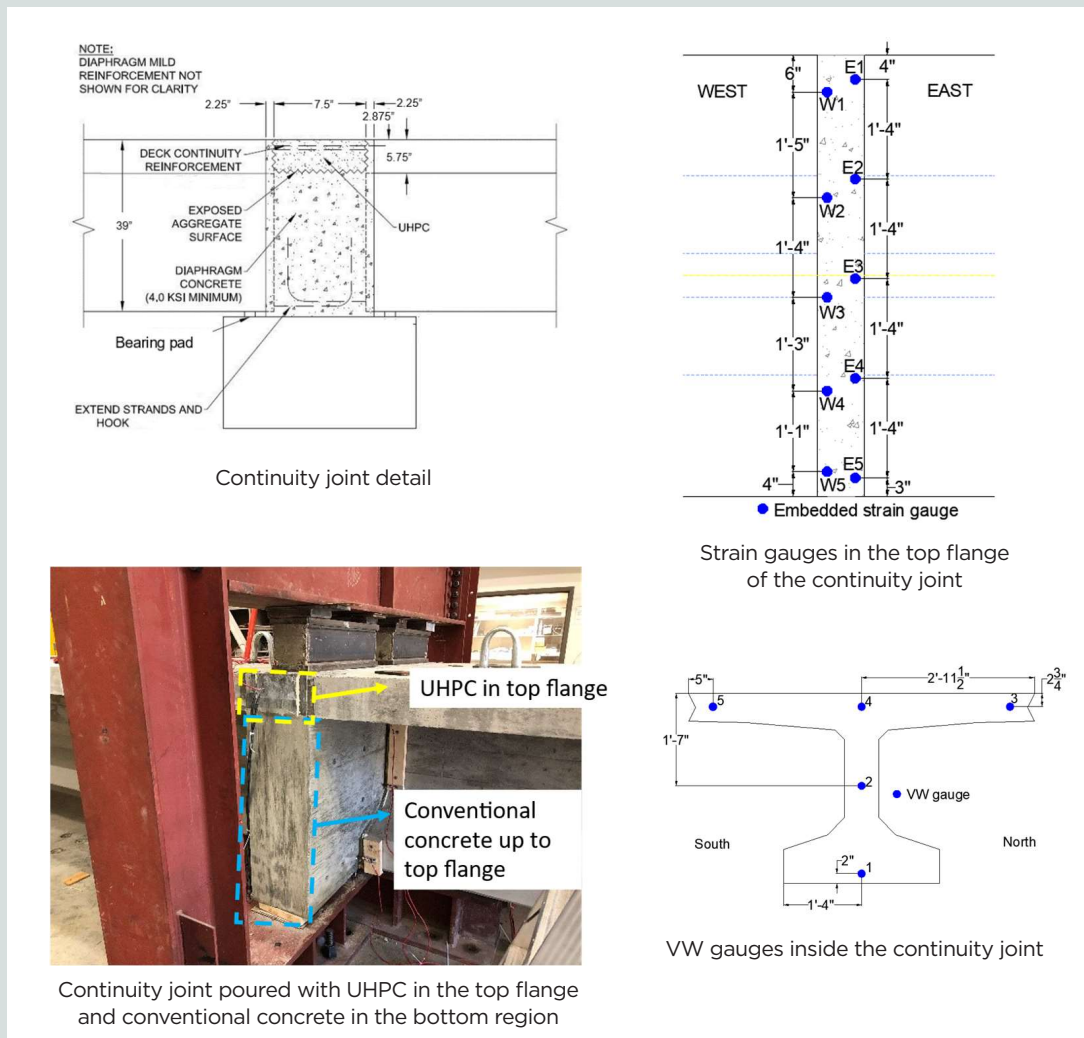


**Figure 12.** Continuity joint test setup details. Note: UHPC = ultra-high-performance concrete; VW = vibrating-wire. 1" = 1 in. = 25.4 mm; 1' = 1 ft = 0.305 m.

**Negative moment testing** To test the joint for negative moment, two frames were erected at 12 ft (3.7 m) on either side of the diaphragm. The east frame was hinged to the top flange of the girder to prevent vertical movement. On the west frame, a hydraulic cylinder was attached to load the diaphragm. **Figure 14** shows the schematics of the test. The temporary support on the west end of the girder was then removed to create a cantilever. The self-weight of the west girder resulted in a negative moment of approximately 230 kip-ft (310 kN-m) at the joint. An additional 114 kip (507 kN) load was applied through the hydraulic cylinder to create another 1311 kip-ft (1777 kN-m) negative moment at the joint. Tensile cracks formed at the top of the continuity joint due to negative moment. Most of the cracking occurred either in the girder flanges or at the interface of the connection. The UHPC did not crack.

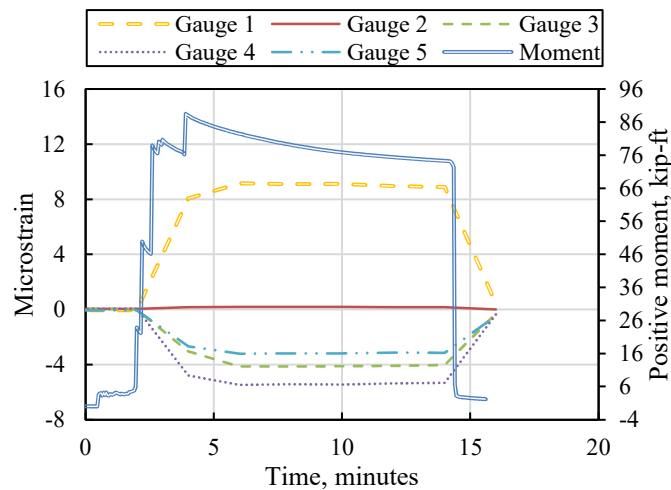
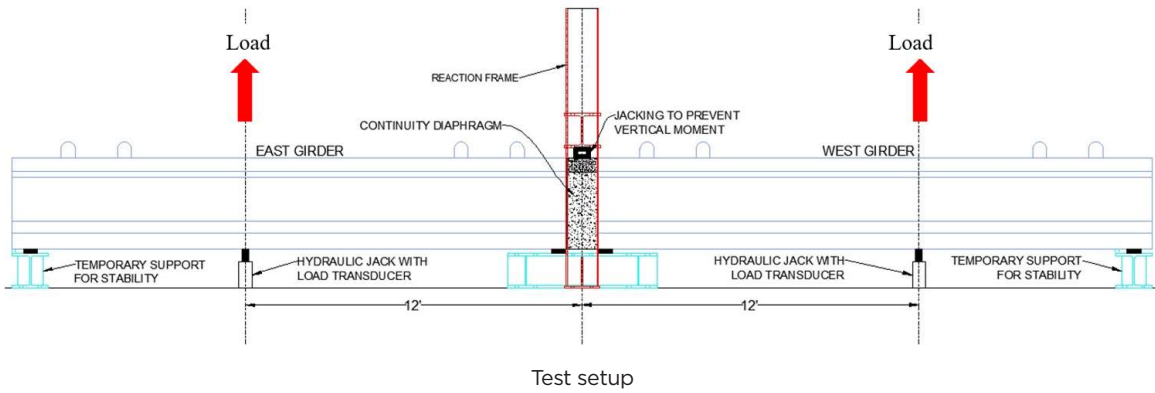
Figure 14 shows strains in the gauges attached to the top-flange reinforcement and embedded in the joint for the east and west girder reinforcement, respectively. At a

load of 98 kip (436 kN) (third-to-last load increment), the strains in both bars at the middle of the joint (W3 and E3) abruptly increased and indicated yielding. The 98 kip load corresponds to a total moment of 1357 kip-ft (1840 kN-m), including the self-weight. This moment exceeded the calculated moment capacity of the joint by 18%. The strain in the reinforcement W2 yielded at the next load increment, but the remaining bars did not indicate yielding even on the final load increment.

## Conclusion

Based on the experimental results, the following observations and general conclusions were made:

- Although cracking in the system tested for combined thermal and fatigue load was not fully discovered until the end of cyclic testing, the authors believe that the cracking occurred early in the thermal cycles. The thermal gradient applied to the system was slight-



Vibrating-wire gauge reading and positive moments at the joint

**Figure 13.** Positive moment testing of the continuity diaphragm. Note: 1' = 1 ft = 0.305 m; 1 kip-ft = 1.356 kN-m.

ly higher than that specified in the AASHTO LRFD specifications and started immediately after UHPC placement. Significant cracking occurred in the second joint pour and minimal cracking occurred in the first joint placement. This finding may be explained by the UHPC gaining sufficient strength in the first joint before thermal-generated strains developed but not gaining enough strength in the second joint before the thermal-generated strains. The flow of UHPC during placement in the second joint was slightly lower than during placement the first joint, which could have affected performance. Although cracking may have existed in the joints, load transfer continued to occur between girders under combined static and thermal load.

- In the system tested for differential camber, cracking was discovered right after the first loading increment was removed from the differential camber leveling. The cracking occurred primarily in the east end of the joints. The UHPC was placed in the east ends last and seemed to have slower flow.

- Though cracking occurred during removal of the differential camber leveling load, crack growth during 1 million load cycles was 1 in. (25.4 mm) or less. In addition, new cracks were not formed during the load cycles.
- The use of UHPC in the longitudinal joints showed promising results as it resulted in simpler joint detailing and continued to transfer load even after cracking. However, more research is required to mitigate thermal cracking of the joints and subsequent leakage.
- The 7.5 in. (191 mm) continuity joint consisting of UHPC in the top 6 in. (150 mm), and conventional concrete in the remaining height of the diaphragm did not show any distress under a positive moment expected from continuity being formed at an age of 28 days.
- The top reinforcement in the continuity joint began to yield at a negative moment more than the calculated negative moment capacity. Additional negative moment caused more bars to yield and resulted in a capacity far exceeding the calculated capacity.

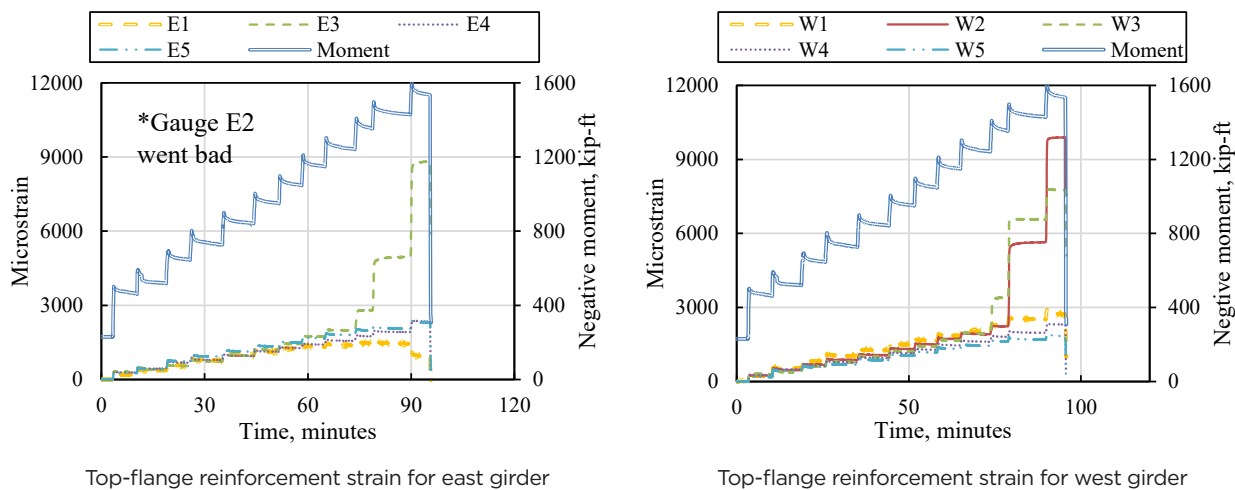
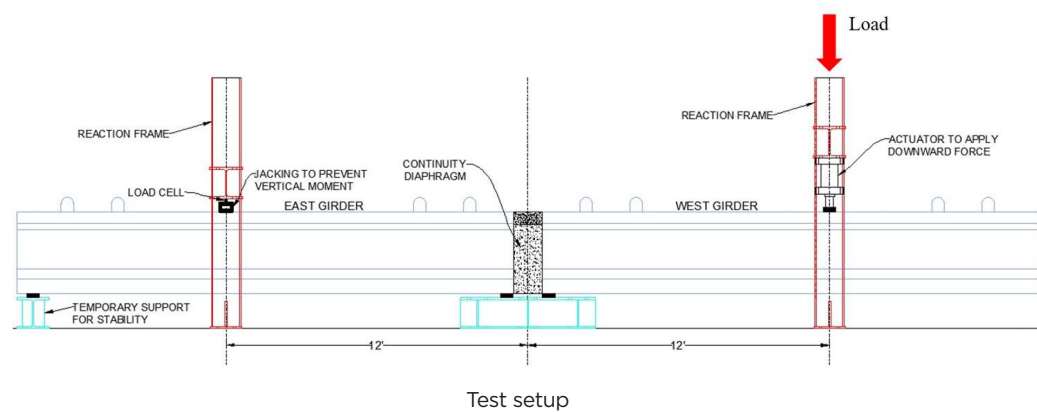


**Figure 14.** Negative moment testing of the continuity diaphragm. Note: 1' = 1 ft = 0.305 m; 1 kip-ft = 1.356 kN-m.

- Using UHPC in the diaphragm can significantly improve the performance of a continuity connection.

## Acknowledgments

The research presented in this paper was a part of National Cooperative Highway Research Program project 18-18, “Design and Construction of Deck Bulb Tee Girder Bridges with UHPC Connections” (see NCHRP report 999 at <https://doi.org/10.17226/26644>). The authors wish to thank the NCHRP project panel and senior program officers Ahmad Abu-Hawash and Waseem Dekelbab for their project oversight and valuable insight and feedback throughout the project. The material presented in this paper is reproduced with permission of the Transportation Research Board. The authors are extremely grateful to the University of Cincinnati lab technician T. J. Brown and the University of Cincinnati graduate students Carlos Tamayo and Sushil Kunwar for their assistance during experimental testing and observations. The authors are also indebted to the UHPC specialist Gregory Nault from LaFarge-Holcim for providing oversight during UHPC placement.

## References

- Stanton, J. F., and A. H. Mattock. 1987. *Load Distribution and Connection Design for Precast Stemmed Multibeam Bridge Superstructures*. NCHRP (National Cooperative Highway Research Project) report 287. Washington DC: Transportation Research Board. [https://onlinepubs.trb.org/Onlinepubs/nchrp/nchrp\\_rpt\\_287.pdf](https://onlinepubs.trb.org/Onlinepubs/nchrp/nchrp_rpt_287.pdf).
- Baer, C. 2013. “Investigation of Longitudinal Joints between Precast Prestressed Deck Bulb Tee Girders Using Latex Modified Concrete.” Master’s thesis, University of South Carolina. <https://scholarcommons.sc.edu/etd/2452>.
- Chapman, C. E. 2010. “Behavior of Precast Bridge Deck Joints with Small Bend Diameter U-Bars.” Master’s thesis, University of Tennessee, Knoxville. [https://trace.tennessee.edu/cgi/viewcontent.cgi?article=1712&context=utk\\_gradthes](https://trace.tennessee.edu/cgi/viewcontent.cgi?article=1712&context=utk_gradthes).
- Li, L., Z. J. Ma, and R. G. Oesterle. 2010. “Improved

- Longitudinal Joint Details in Decked Bulb Tees for Accelerated Bridge Construction: Fatigue Evaluation.” *Journal of Bridge Engineering* 15 (5): 511–522. [https://doi.org/10.1061/\(asce\)be.1943-5592.0000097](https://doi.org/10.1061/(asce)be.1943-5592.0000097).
5. French, C., C. Shield, D. Klaseus, M. Smith, W. Eriksson, Z. Ma, P. Zhu, S. Lewis, and C. Chapman. 2011. *Cast-in-Place Concrete Connections for Precast Deck Systems*. NCHRP Web-Only Document 173. Washington, DC: Transportation Research Board. <https://doi.org/10.17226/17643>.
  6. ACI (American Concrete Institute) Committee 318. 2019. *Building Code Requirements for Structural Concrete (ACI 318-19) and Commentary*. Farmington Hills, MI: ACI.
  7. Miller, R. A., G. M. Hlavacs, T. Long, and A. Greuel. 1999. “Full-Scale Testing of Shear Keys for Adjacent Box Girder Bridges.” *PCI Journal* 44 (6): 80–90. <https://doi.org/10.15554/pcij.11011999.80.90>.
  8. Sharpe, G. P. 2007. “Reflective Cracking of Shear Keys in Multi-Beam Bridges.” Master’s thesis, Texas A&M University. <http://oaktrust.library.tamu.edu/bitstream/handle/1969.1/ETD-TAMU-1912/SHARPE-THESIS.pdf?sequence=1>.
  9. Grace, N. F., E. A. Jensen, and M. R. Bebawy. 2012. “Transverse Post-Tensioning Arrangement for Side-by-Side Box-Beam Bridges.” *PCI Journal* 57 (2): 48–63. <https://doi.org/10.15554/PCIJ.03012012.48.63>.
  10. Hussein, H. H., S. M. Sargand, F. T. Al Rikabi, and E. P. Steinberg. 2017. “Laboratory Evaluation of Ultrahigh-Performance Concrete Shear Key for Prestressed Adjacent Precast Concrete Box Girder Bridges.” *Journal of Bridge Engineering* 22 (2): 04016113. [https://doi.org/10.1061/\(asce\)be.1943-5592.0000987](https://doi.org/10.1061/(asce)be.1943-5592.0000987).
  11. Graybeal, B. A., and J. L. Hartman. 2003. “Ultra-High Performance Concrete Material Properties.” Paper presented at the 2003 Transportation Research Board Conference. [https://www.researchgate.net/publication/312461906\\_Ultra-high\\_performance\\_concrete\\_material\\_properties](https://www.researchgate.net/publication/312461906_Ultra-high_performance_concrete_material_properties).
  12. Rapoport, J., C.-M. Aldea, S. P. Shah, B. Ankenman, and A. Karr. 2002. “Permeability of Cracked Steel Fiber-Reinforced Concrete.” *Journal of Materials in Civil Engineering* 14 (4): 355–358. [https://doi.org/10.1061/\(ASCE\)0899-1561\(2002\)14:4\(355\)](https://doi.org/10.1061/(ASCE)0899-1561(2002)14:4(355)).
  13. Graybeal, B. 2014. *Design and Construction of Field-Cast UHPC Connections*. FHWA-HRT-14-084. Washington, DC: Federal Highway Administration. <https://www.fhwa.dot.gov/publications/research/infrastructure/structures/14084/14084.pdf>.
  14. Haroon, A., H. Waleed, E. Steinberg, K. Walsh, R. Miller, and B. Shahrooz. “Investigating UHPC in Deck Bulb-Tee Girder Connections, Part 1: Analytical Investigation.” *PCI Journal* 68 (3): 62–78. <https://doi.org/10.15554/pcij68.3-04>.
  15. AASHTO (American Association of State Highway and Transportation Officials). 2020. *AASHTO LRFD Bridge Design Specifications*. 9th ed. Washington, DC: AASHTO.
  16. Shi, W., B. Shafei, Z. Liu, and B. M. Phares. 2019. “Early-Age Performance of Longitudinal Bridge Joints Made with Shrinkage-Compensating Cement Concrete.” *Engineering Structures* 197: 109391. <https://doi.org/10.1016/j.engstruct.2019.109391>.
  17. Miller, R., B. Shahrooz, A. Haroon, E. Steinberg, W. Hamid, A. Chlost, and C. Slyh. Forthcoming. *Proposed AASHTO Guidelines for Adjacent Precast Concrete Box Beam Bridge Systems*. NCHRP research report 1026. Washington DC: Transportation Research Board.

## Notation

- $T_1$  = thermal gradient between girder surface and 16 in. depth
- $T_2$  = thermal gradient between 4 in. and 16 in. depths

## About the authors



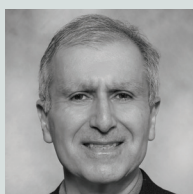
Abdullah Haroon is a graduate research assistant in the Department of Civil and Environmental Engineering at the University of Cincinnati in Ohio.



Eric Steinberg, PhD, PE, is a professor in the Department of Civil Engineering at the Ohio University in Athens.



Richard Miller, PhD, PE, is a professor in the Department of Civil and Environmental Engineering at the University of Cincinnati.



Bahram Shahrooz, PhD, PE, is a professor in the Department of Civil and Environmental Engineering at the University of Cincinnati.



Waleed Hamid, PhD, is a faculty member in the Department of Construction and Projects at the University of Fallujah in Iraq.

## Abstract

Deck bulb-tee girders constitute an excellent precast concrete bridge element system for medium- to long-span bridges. The precast concrete girders are transported to the jobsite, where they are placed adjacent to each other. The girders are connected using field-cast longitudinal joints. When required, a continuity diaphragm over the pier is used to create moment continuity; however, there is a risk of cracking of the field-cast joints and construction can be difficult when adjacent girders have different camber profiles. Given these challenges, adoption of the deck bulb-tee girder systems has been limited.

Analytical investigation performed in part 1 of this series of papers indicated that using ultra-high-performance concrete (UHPC) can improve the performance of the field-cast joints and help overcome construction difficulties. This paper describes full-scale experimental testing performed as a follow-up to the analytical investigation. Longitudinal joints grouted with UHPC were tested under a combination of thermal and live load. A continuity diaphragm with partial UHPC was also tested under positive and negative moments over the pier.

## Keywords

ABC, accelerated bridge construction, bulb-tee girder, connection, girder, UHPC, ultra-high-performance concrete.

## Review policy

This paper was reviewed in accordance with the Precast/Prestressed Concrete Institute's peer-review process. The Precast/Prestressed Concrete Institute is not responsible for statements made by authors of papers in *PCI Journal*. No payment is offered.

## Publishing details

This paper appears in *PCI Journal* (ISSN 0887-9672) V. 68, No.4, July–August 2023, and can be found at <https://doi.org/10.15554/pcij68.4-01>. *PCI Journal* is published bimonthly by the Precast/Prestressed Concrete Institute, 8770 W. Bryn Mawr Ave., Suite 1150, Chicago, IL 60631. Copyright © 2023, Precast/Prestressed Concrete Institute.

## Reader comments

Please address any reader comments to *PCI Journal* editor-in-chief Tom Klemens at [tklemens@pci.org](mailto:tklemens@pci.org) or Precast/Prestressed Concrete Institute, c/o *PCI Journal*, 8770 W. Bryn Mawr Ave., Suite 1150, Chicago, IL 60631. 